Conditions for Surf-riding in an Irregular Seaway

K. J. Spyrou, *National Technical University of Athens*, spyrou@deslab.ntyua.gr
V. Belenky, *David Taylor Model Basin, Carderock, Washington D.C.*
N. Themelis, *National Technical University of Athens*, nthemelis@naval.ntua.gr
K. Weems, *Science Applications International Corporation*

ABSTRACT

The current study is motivated by a desire to evaluate the probability of surf-riding in irregular seas by posing surf-riding as a threshold-exceedance problem. For steep regular following waves, it is known that celerity is the speed at which, if exceeded by a ship, capture into surf-riding is necessarily incurred. Can this simple phenomenological rule be extended to a stochastic wave environment? To answer this, a suitable definition of wave celerity for an irregular seaway needs to be put forward. In the current work we define celerity as the velocity of propagation of a suitable property of the profile. This leads to the concept of instantaneous celerity which opens a window towards the literature of instantaneous frequency in signal processing. In general, instantaneous celerity cannot be consistently defined as a smooth and constrained curve. Other definitions of local (but not instantaneous) celerity are also possible. In the paper we test these for a number of different selections, obtaining time-dependent celerity curves for various types of waves and we assess the effect of spectrum's band-width, relaxing the requirement of "narrow-bandness". Subsequently we implement simultaneous treatment of the "wave" and "ship" processes and we investigate the potential of applying a local celerity condition for surf-riding prediction. Various patterns of behaviour before and into surf-riding are observed and discussed.

Keywords: *Surf-riding, Wave Celerity, Irregular Waves*

1. INTRODUCTION

In developing a probabilistic evaluation of a ship's tendency for surf-riding, a significant challenge lies in the definition of wave celerity for an irregular sea environment. Specifically, it is not known if some notion of wave velocity pertaining to a multi-frequency wave profile could be used as an unambiguous threshold speed for the prediction of surf-riding, in the same fashion that celerity is used for a regular sea. One sort of statistical celerity would be the so-called "drift velocity," a deterministic quantity based on the ratio of the average wave length to the average wave period. Under the assumption of a Gaussian distribution of wave elevation, Longuet-Higgins (1957) derived approximate closed-form expressions of the velocity distribution for the maxima and minima that appear on a plane (vertical) section of the profile of a short-crested sea. Given a spectrum, the velocity distributions of the so-called "specular points" of the profile, where the gradients in the two directions of wave propagation match desired constant values, can also be obtained. More recent elaborations on the velocity distributions of various points of random wave surfaces are described in Baxevani et al. (2003), in Aberg and Rychlik (2006, 2007), and elsewhere. In a study that aimed to calculate the probability of encounter of waves that could cause broaching-to, Aberg and Rychlik (2007) selected the "wave centre" (the point of downward zero-crossing) for defining wave velocity in a Gaussian sea. Its distribution was derived for both fixed and moving (with constant speed) observers by using Rice's formula. They also discussed a celerity distribution based on the half wave length for an approximate, deterministic, dispersion relationship.

Unfortunately, a statistical model of celerity is of limited use for deriving the probability of surf-riding. The process of the difference between celerity and ship speed becomes strongly nonlinear for the parameters' range of interest. Hence, the exact role of celerity for surf-riding in an irregular sea needs to be clarified. Extra details about the context of the discussed problem are found in a companion paper by Belenky et al. (2012).

2. EQUATION OF SHIP MOTION

Consider a wave profile in time and unidirectional space, as follows:

$$\zeta(x;t) = \int_0^\infty \sin\left(kx - \omega t + \varepsilon^{(r)}(\omega)\right)\sqrt{2S(\omega)d\omega} =$$
$$= \sum_{i=1}^{n} A_i \sin\left[k_i(x - c_i t) + \varepsilon_i^{(r)}\right] \qquad (1)$$

where ζ is the elevation above still water, x is the distance of the considered point of the profile from an earth-fixed origin and t is the corresponding time instant; ω, k are the wave frequency and wave number, respectively; $\varepsilon^{(r)}$ is the random phase; A_i, k_i, c_i and $\varepsilon_i^{(r)}$ are the wave amplitude, number, celerity, and phase, respectively, of the discrete wave component with frequency ω_i; and $S(\omega)$ is the wave spectrum. The well-known dispersion relation $\omega = \sqrt{gk}$ for each harmonic wave component propagating in deep water is applied. The superscript (r) indicates a random number, uniformly distributed in $[0,2\pi]$ which specifies the phase of each harmonic component at $t = x = 0$. Note that the "neat" integral representation of the elevation in eq. (1) is not a Riemann-type integral (Pierson 1955; see also discussion in Kinsman 1984).

For a shore-based observer, a basic model of the ship surge motion in this wave could be written as follows (Spyrou 2006):

$$\underbrace{(m - X_{\dot{u}})\ddot{\xi}}_{inertia\ M(\ddot{\xi})} - \underbrace{\left(\tau_2\dot{\xi}^2 + \tau_1 n\,\dot{\xi} + \tau_0 n^2\right)}_{thrust\ T(\dot{\xi};n)} + \underbrace{\left(r_1\dot{\xi} + r_2\dot{\xi}^2 + r_3\dot{\xi}^3\right)}_{resistance\ R(\dot{\xi})} +$$
$$+ \underbrace{\int_0^\infty \cos\left[\frac{\omega^2}{g}\xi - \omega t + \varepsilon^{(r)}(\omega) + \varepsilon_f(\omega)\right] X_w(\omega)\sqrt{2S(\omega)d\omega}}_{wave\ force\ F(\xi;t)} = 0 \qquad (2)$$

where ξ is the instantaneous longitudinal position of the origin of the ship axes; m, and $X_{\dot{u}}$ are the ship's mass and added mass, respectively; n is propeller's rotation rate; and $X_w(\omega)$ and $\varepsilon_f(\omega)$ are the RAO and phase of linear wave surging force corresponding to the ω harmonic wave. After approximating the wave force by a large, but finite, sum of discrete harmonic components, this equation can be expressed, with some rearrangement, as:

$$(m - X_{\dot{u}})\ddot{\xi} + r_3\dot{\xi}^3 + (r_2 - \tau_2)\dot{\xi}^2 + (r_1 - \tau_1\eta)\,\dot{\xi} +$$
$$+ \sum_{i=1}^{n} f_i \cos\left[k_i\xi - \omega_i t + \varepsilon_i^{(r)} + \varepsilon_{f_i}\right] = \tau_0 n^2 \qquad (3)$$

This equation depends explicitly on time t, as for parametrically excited systems. The t dependency can be removed for a regular (monochromatic) sea through a coordinate transformation. But this does not seem to be possible for an irregular sea.

3. INSTANTANEOUS CELERITY FOR GAUSSIAN FORMULATION

When the wave profile is irregular, the frequency and wave number change continually. At first consideration, one might think of an expression of celerity by extending the deterministic relation of the frequency over the wave number. However, this requires meaningful definitions of the localized wave frequency in space and in time. One could extract such quantities by applying a short-time Fourier or by processing the wave profile simultaneously in the time and "frequency" domains by a continuous wavelet transform. However, due to the renowned problem of resolution when the time duration of the considered signal's segment is very short [there can be either temporal or spectral localization, but not both (Gabor limit); see Gabor (1946)] these approaches are ineffective. In signal processing, the idea of "instantaneous frequency" was introduced many years ago, but has yet to gain universal acceptance – for a review see Boashash (1992). The matter acquires greater importance for non-stationary signals. The Fourier transform is incongruent with the notion of "instantaneous" frequency. The latter is considered by some as a quantity with a different nature, and questions have been raised as to which of the two is actually measured during experiments. Mandel (1974) claimed that the only similarity between the two versions of frequency is that the average frequency of a spectrum derived by the Fourier transform is equal to the time average of the instantaneous frequency. While these ideas determine a possible way to attack the problem, a more direct approach is preferred here.

The mapping of wave phase to the local gradient of the profile is not as apparent as in the periodic case. A quite generic notion could be that celerity is the rate at which some derivative of the wave function is propagated. Since the selection of the propagated property (as well as its quantitative value) may result in different values of celerity, even for a short segment of an irregular profile, in principle such a selection can be tailored to the specific problem of interest. Longuet-Higgins (1957) presented definitions of "velocities of zeros" based on a fixed value of the elevation ζ or of the gradient $\frac{\partial \zeta}{\partial x}$ as follows: consider a function h determined from the wave profile that obtains the value h_0 at $(x_0; t_0)$. On the locus of $h = h_0$ the differential dh is naught by definition, leading to an expression of velocity:

$$dh = h_0 - h_0 = 0 = \frac{\partial h}{\partial x} dx + \frac{\partial h}{\partial t} dt \quad \rightarrow \quad c_{h_0} = -\frac{\partial h}{\partial t} \Big/ \frac{\partial h}{\partial x} \tag{4}$$

For a deep water wave elevation process represented by a large (theoretically infinite) sum of harmonics waves as described by equation (1), consider a point on the wave profile corresponding to a frozen time instant t_0 and located at a longitudinal distance x_0 from the origin. The instantaneous local wave slope is:

$$\left.\frac{\partial \zeta(x;t_0)}{\partial x}\right|_{x_0} \equiv a(x_0;t_0) = \sum_{i=1}^{n} \sqrt{2S(\omega_i)\delta\omega}\, k_i \cos\left[k_i(x_0 - c_i t_0) + \varepsilon_i^{(r)}\right] \tag{5}$$

It is possible to trace the locus $x_a(t)$ by marching in time, solving equation (5) numerically for a series of time steps following t_0. In the first time step, for instance, equation (6) below would be solved to get δx, given a δt (the reverse is in fact computationally more efficient – such cases are encountered later):

$$\sum_{i=1}^{n} A_i k_i \cos\left[k_i\left[x_0 + \delta x - c_i(t_0 + \delta t)\right] + \varepsilon_i^{(r)}\right] = \alpha(x_0;t_0) \tag{6}$$

For subsequent steps, the solution $x_0 + \delta x$ will replace x_0 while $t_0 + \delta t$ will replace t_0 and the next nearby solution will be identified. Eventually a series solution is traced:

$$x_a(t) = f(t;a)|_{x_0, t_0} \tag{7}$$

where the subscript on the right-hand side indicates the starting point of the iterative solution process. The time derivative of $x_a(t)$ should produce a "local" celerity function uniquely associated with each pair (x_a, t):

$$c_a(t) = \dot{x}_a(x;t) = \frac{df(t;a)}{dt} \tag{8}$$

For irregular waves, this local velocity is time-varying. Furthermore, a different celerity value should, in principle, be expected for each point of a profile within an apparent length (e.g. between successive up-crossings).

Following Longuet-Higgins more closely, it is also possible to base celerity on a fixed value of the spatial gradient $h = \frac{\partial \zeta(x;t)}{\partial x}$:

$$c(x,t) = \frac{\frac{\partial^2 \zeta}{\partial x\, \partial t}}{\frac{\partial^2 \zeta}{\partial x^2}} \tag{9}$$

Note that this expression is not tied to a specific slope value (hence no subscript a), thus producing a celerity value from an instantaneous position and time.

Approximate calculations of celerity in an irregular seaway might also be contemplated. For example, consider a pair (x, t) that defines a point of the irregular profile in space and time. Fix t and measure the distance between the crests (local maxima) that are found just before and just after x, calling this distance $\tilde{\lambda}$. Subsequently, fix x and measure the corresponding distance of crests in the time domain (just before and just after the considered instant t), noting it as $\tilde{T}$. This alternative definition of celerity leads to the expression:

$$\tilde{c} = \frac{\tilde{\lambda}}{\tilde{T}} \tag{10}$$

One should recall here that counting distances between crossings (e.g. up-crossings) could lead to a substantially different result for a wave spectrum that is not very narrow-banded. A feature of irregular waves is that individual crests (or troughs) can emerge or vanish. Naval architects have known for many years that they need to cope with such phenomena, e.g. see Vossers 1962; yet the issue is rarely touched, since in most cases the assumption of a narrow band wave spectrum underlies the calculation process. For "Gaussian" elevations, the ratio of the number of zero crossings N_0 to the number of crest and troughs N_1 is defined as follows:

$$\frac{N_0}{N_1} = \sqrt{1 - \varepsilon^2} \tag{11}$$

In this case, ε is the spectrum's width, with no relation with the phase symbol ε. The generation of troughs with positive elevation as well as of troughs with negative elevation, are phenomena that are expected to make celerity behave in a strongly nonlinear fashion from time to time. The implementation of this definition of celerity is evaluated next for three different characteristic cases.

Example 1

For the first example, consider a wave comprised of three frequencies at "some distance" from each other, as defined in Table 1. The waves are selected to be reasonably steep, yet linear. Figure 1 plots the wave profile in space–time. Merging and separation of waves is observed. Such qualitative changes in the wave profile should be reflected in a sharp change of the value of celerity. At some times, more than one crest may be found between an up-crossing and the successive down-crossing (e.g. two crests with a trough of positive elevation between them). This is the reason for the ratio of equation (11) to become less than 1.

Table 1: Selected linear wave components

k [m^{-1}]	0.1	0.05	0.14
$\omega = \sqrt{gk}$ [s^{-1}]	0.99	0.70	1.17
A [m]	1.0	1.4	0.6
Ak	0.1	0.07	0.084
$\varphi = kx - \omega t + \varepsilon$	0.1	0.8	0.5

Figure 2 shows several loci of solutions $x_a(t)$ as defined in equation (7). Curves of similar nature are presented in Sjo (2000), drawn for zero crossing points (these points do not maintain the slope). Recalling that the celerity that corresponds to any one point of these curves is given by the gradient dx_a/dt at that point of the curve, x_a is traced versus t in order to find the locus of points for four different local wave slope values: 0 (i.e. a crest or a trough), 0.0125, 0.025 and 0.05. The solutions are presented in Figure 2 as bunches of four contour lines, with one line per value of slope. Note that, at any time instant, each value of slope can be realised several times, so there are several families of solutions.

In contrast to a periodic wave case, these constant slope lines are neither straight nor parallel to one another. While the gradient, and thus celerity, is mostly not changing much, there are "strange" regions that basically correspond to the merging of crests. Note in particular the backward turn of some lines – corresponding to the more extreme value of local wave slope 0.05 – that leads to their unification with the corresponding curve of the previous group. It reflects the fact that in the considered wave cycle this value of wave slope was not realized – i.e. the wave was not steep enough. The annihilation (or creation) of such points of constant slope is referred to as "twinkle" (Kratz and Leon 2005).

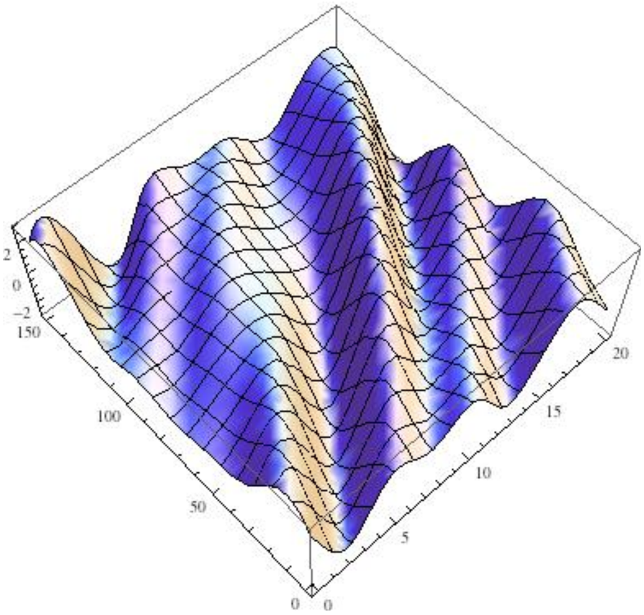

Figure 1: Example 1 wave in space-time.

Example 2

Now consider a wave elevation process defined by the JONSWAP spectrum (Figure 3). This spectrum was discretised using 15 frequencies distributed equidistantly between 0.63 and 1.43 of the peak value. For the prescribed range, the bandwidth parameter ε receives the rather moderate value of 0.315. Sample realisations are plotted in Figure 4. Figure 5 shows contours of slope 0.0 (crests and troughs) as well as slope 0.01 as traced using the solution of $x_{a=0}(t) = f(t;0)|_{x_0,0}$.

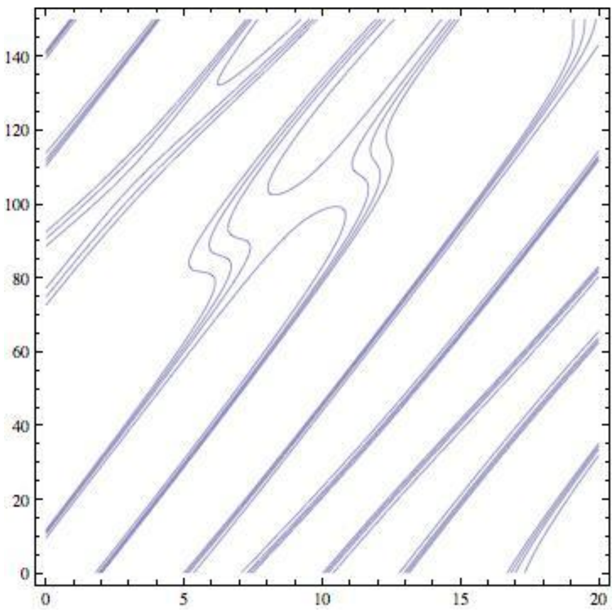

Figure 2: Constant slope contours from the solution of eq. (7), for the three-frequency wave considered as Example 1. The slopes are 0, 0.0125, 0.025 and 0.05. Above the main diagonal, wave slope increases downwards; below it, the increase is upwards.

The celerity curve produced by propagating the first crest that lies right in front of the axes origin is shown in Figure 6. Similar celerity curves referring to the third crest are shown in Figure 7. Table 2 specifies the initial ($t = 0$) ordinates of these points. The variability of celerity is prevalent and spikes are noted. These indicate singular behaviour where and when a relatively steep slope disappears and, as a result, velocity jumps to infinity. This phenomenon has, of course, also been observed before (see for example Baxevani et al. 2003). While the curve could be smoothed or clipped, evaluation of its importance is required.

Finally, the calculated local celerity value is compared to one obtained by applying the approximate expression $\tilde{c} = \tilde{\lambda}/\tilde{T}$. The length and period used for this calculation are explained in Figure 8. The "exact" and approximate values of celerity are compared for two different slope values in Figures 9 and 10. A second alternative celerity calculation was also tested, based on the ratio of apparent half-length to apparent half-period. These quantities are measured between successive peaks in time and in space, observed before and after a given point (x, t). This second alternative (also plotted in Figures 9 and 10) seems to be a consistently superior predictor. Such a conclusion is deduced if one compares the position of unfilled squares against the continuous line; and similarly, that of the unfilled circles against the dashed line. It is noted that a similar comparison for the filled symbols (that are based on whole lengths and periods) revealed much larger discrepancies. The examination of other points of the profile gave similar results.

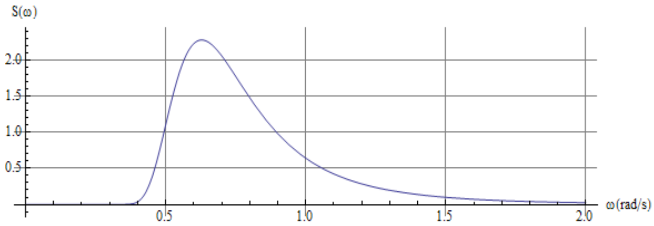

Figure 3: JONSWAP spectrum for H_S = 4 m, T_P = 10 s (generalized Philip's constant a_w = 0.00809 and peakedness parameter γ = 1).

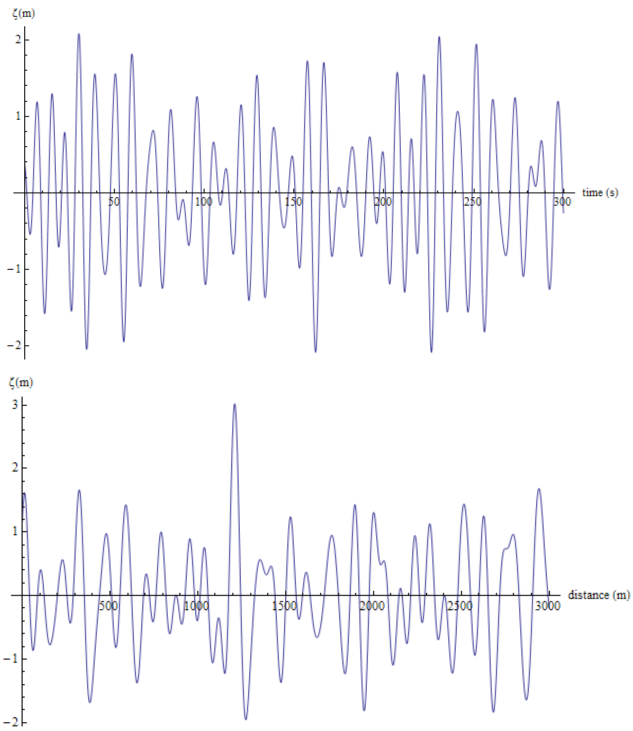

Figure 4: Wave elevations at x = 100 m (top) and for t = 0 s (bottom).

Table 2: Location of propagated wave profile points at t = 0 s.

Slope	x_0 (m)	
	Around Crest 1	Around Crest 3
0	13.23	229.53
1/100	11.47	224.12
1/75	10.87	222.07
-1/100	15.01	234.51
-1/75	15.61	236.18

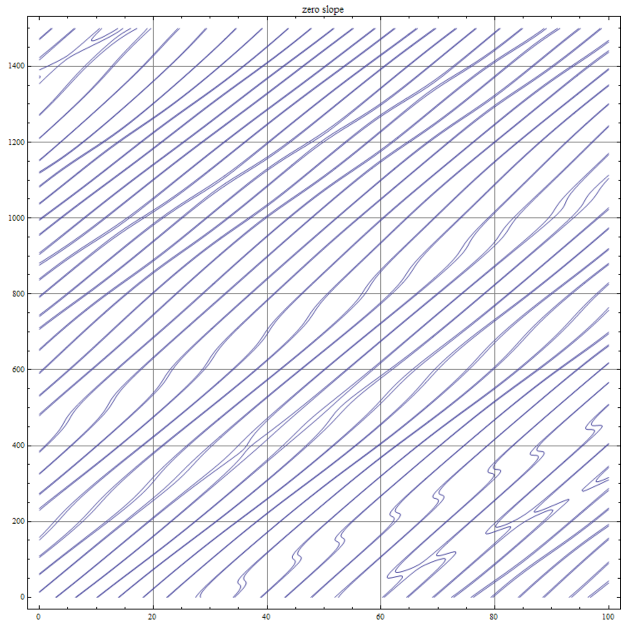

Figure 5: Contour plots for slopes a = 0, 0.01.

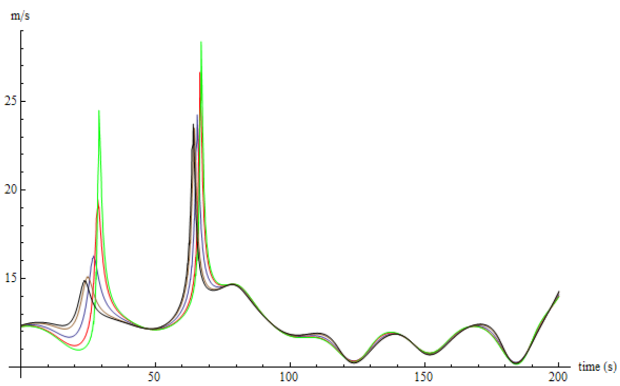

Figure 6: Celerity curves corresponding to wave slopes 1/75, 1/100, 0, -1/100, -1/75 (initially in vicinity of first crest).

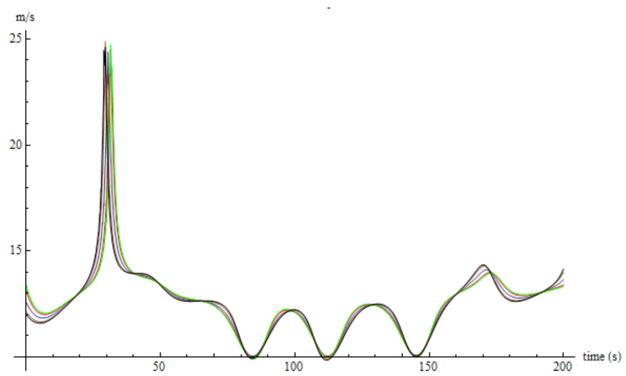

Figure 7: Wave velocity curves for the third crest.

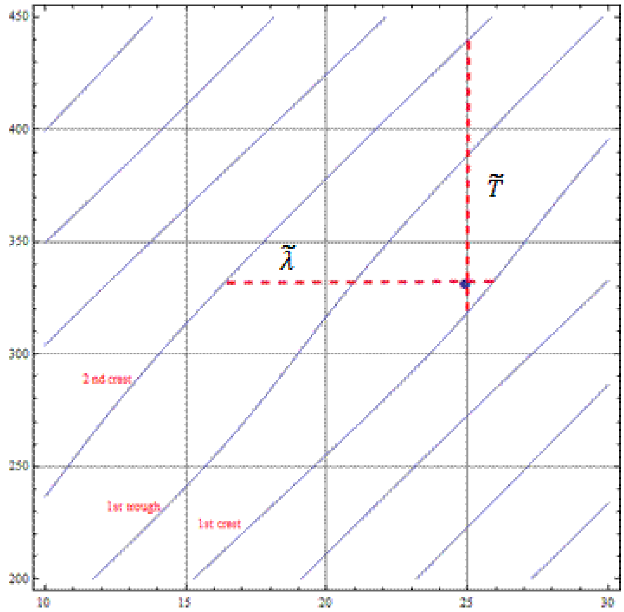

Figure 8: Wave length and wave period used for the approximate calculation of celerity. The dashed lines are measured between crests and the dotted lines between a crest and a trough.

<u>Example 3</u>

For the third example, the same JONSWAP spectrum was assumed. However, only a few frequencies around the peak were used this time. The considered spectral area was enlarged in successive runs in order to have bandwidth as the free parameter (Figure 11).

The celerity curve corresponding to the first crest after the origin is derived for three realisations of each bandwidth and plotted in Figure 12. The three realisations differ only in the (random) phases. As expected, the variability of celerity in time is intensified as the bandwidth goes up. This trend is consistent for all considered samples.

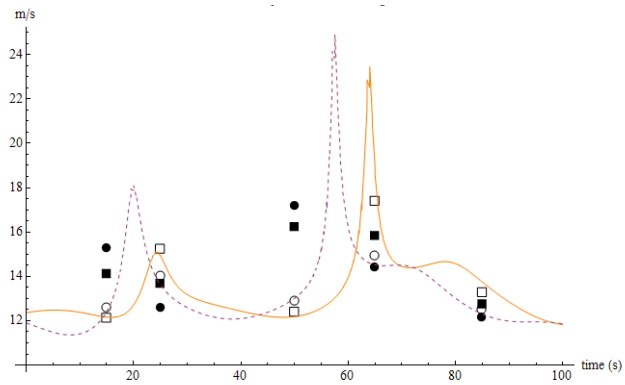

Figure 9: Comparison of the velocities obtained by propagating the first pair of points with slope a = -1/100 (see Table 2). The dashed line shows the celerity of the first point on the down-slope with slope a (nearer to crest). The continuous line is for the second point (nearer to trough). Each unfilled symbol refers to distance between successive peaks at the specified instant of time (position is implied). Filled symbols refer to distance between successive crests. Circles refer to the higher point (after the crest) and rectangles to the lower (before the trough).

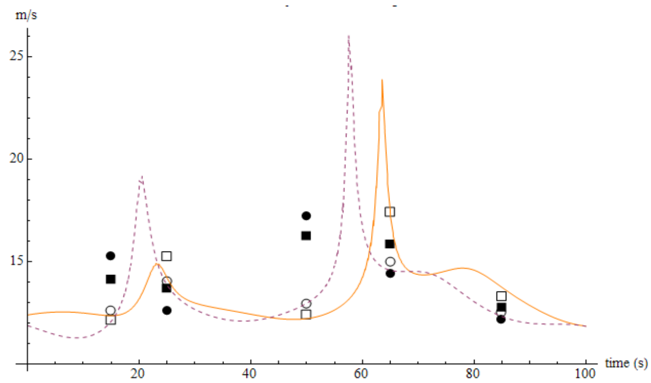

Figure 10: Comparison of velocities similar to Figure 9, but for a = -1/75.

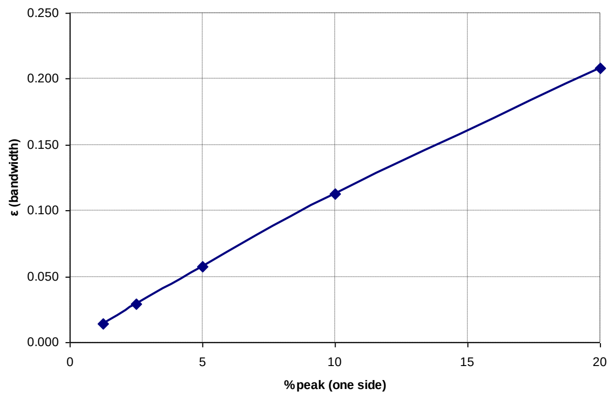

Figure 11: Example 3 spectrum bandwidths.

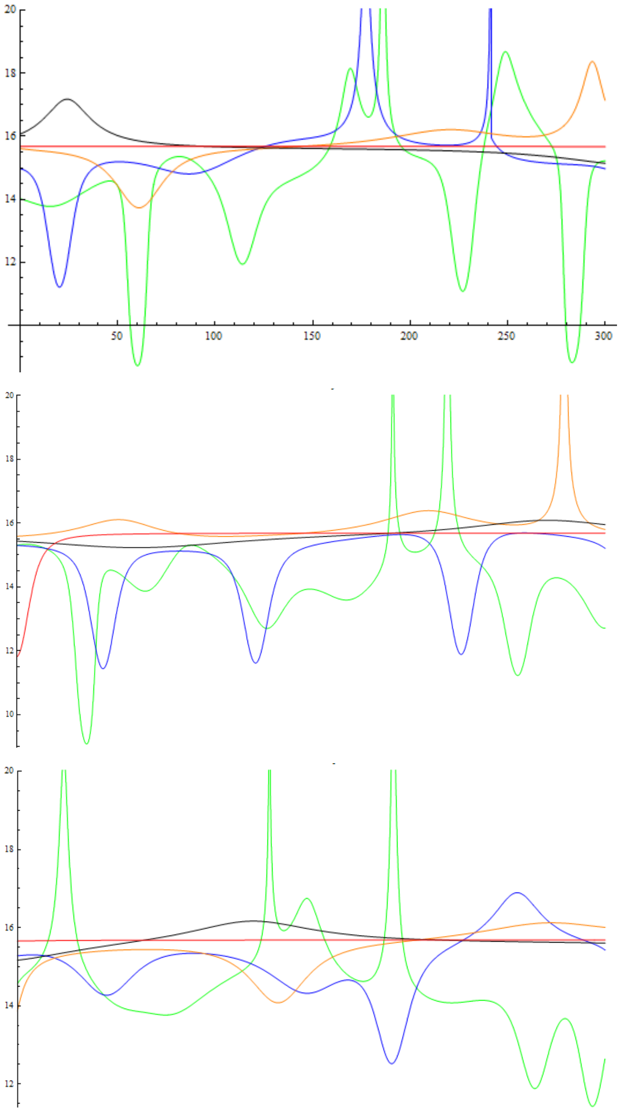

Figure 12: Celerity curves obtained by propagating the first crest for five different bandwidths. The three diagrams differ only in the random phases of the component waves. Red curves correspond to 1.25% of peak period on each side, black 2.5%, orange 5%, blue 10% and green 20%.

4. CELERITY DEFINITION FOR SURF-RIDING ASSESSMENT

The definition of instantaneous celerity suffers from a number of drawbacks. First, no matter what slope value is selected, there will be apparent wave cycles where any given value will not be realized. However, these waves will not be particularly steep and thus are unlikely to create surf-riding. The spikes, which are points where celerity jumps to infinity because of the annihilation of the points with the considered slope value, seem to present a more critical problem.

Another definition of a local (but not instantaneous) celerity that could be tried is based on the steepest point on the down slope of the wave profile that is nearest to the ship. Such a choice has an advantage because it is likely to be closely related to the maximum of the Froude-Krylov surge force acting on the ship, which is well known to have a critical connection with the occurrence of surf-riding. Often, maximum wave force and maximum slope are realized with a small phase difference. Computational burden is not substantially different between the point of maximum wave slope or maximum wave force. However, the first is a local wave characteristic that is in a physical context observable.

At least one point of maximum slope can be found on the down slope of every apparent cycle, yet it can degenerate to zero slope if its vicinity (e.g. its distance from the neighbouring crest) shrinks to a zero length. However, it is believed that such encounters represent relatively mild conditions for the ship and such singular points should therefore be unimportant for the surf-riding probability calculation. For a relatively narrow band sea, such events should be rare. It should be noted that there can be more than one point of locally maximum slope on a down slope.

As a ship advances with respect to a wave profile or the wave profile overtakes the ship, the targeted nearest point of maximum slope will change in a discrete stepped manner at least once every apparent encounter period. The obtained celerity curve will therefore present points of discontinuity with step-wise change.

In order to calculate the celerity based on the propagation of the point of max slope in the vicinity of the ship, let $\xi(t)$ be the ship's position at some arbitrary time instant t, and search for points of max wave slope that lie near to $\xi(t)$ and are on the down slope. The following equation is solved for $x_{a_{max}} = f(t;\, a_{max})$, using Newton iterations started from the current position of the ship $\xi(t)$:

$$\frac{\partial^2 \zeta(x_{a_{max}}, t)}{\partial x^2} = 0 \qquad (12)$$

Simultaneously, the following inequality should be satisfied to ensure that the point is on the down slope:

$$\frac{\partial^3 \zeta(x_{a_{max}},\ t)}{\partial x^3} < 0 \qquad (13)$$

For a 4th order finite difference approximation of the derivative, k more points are determined, separated by a time interval δt:

$$\frac{\partial^2 \zeta(x_{a_{max}}, t+\delta t)}{\partial x^2} = 0 \;\rightarrow\; x^{(k)}_{a_{max}} = f(t + k \cdot \delta t;\ a_{max}) \qquad (14)$$

Since the time step δt is selected to be very small, the same initial guess $\xi(t)$ should practically suffice unless the initial point is very near to one of the special points mentioned earlier, where a stepped change takes place. Thereafter the celerity can be approximated by the formula:

$$c^{(4)} = \frac{-x^{(2)}_{a_{max}} + 8x^{(1)}_{a_{max}} - 8x^{(-1)}_{a_{max}} + x^{(-2)}_{a_{max}}}{12\ \delta t} \qquad (15)$$

In order to ensure that the located points truly lie near the ship, the following inequality condition can also be imposed on the solution

$$x^{(k)}_{a_{max}} : \left| x^{(k)}_{a_{max}} - \xi(t) \right| < d \qquad (16)$$

where d can be a suitable fraction of the instantaneous wave length.

In the analysis of ship motion data, the celerity is calculated for each time step of the simulation time history by tracking the point of maximum wave slope nearest this ship at that time. The examples below demonstrate the tracking scheme for simulations of the tumble-home ship from the ONR Topside series (L=154 m) in regular, bichromatic and irregular waves. In these examples, the simulation time step $\Delta t = 1$ while the tracking time interval $\delta t = 10^{-3}$.

<u>Example 4</u>

Here the scheme is applied for a simulation in regular waves in order to verify that the known regular wave celerity is captured (Figure 13).

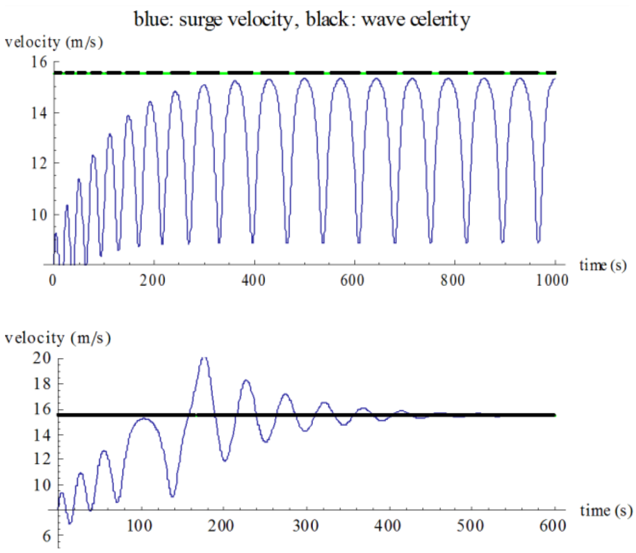

Figure 13: Surging versus celerity for:
ζ_1 = 3.8 m, λ = 154 m, Fn = 0.295 (upper),
ζ_1 = 3.8 m, λ = 154 m, Fn = 0.324 (lower).

The calculated celerity curve appears in Figure 13 as a dashed line. In this initial implementation, the procedure is to find a maximum slope point by iterating to solve Equation (12) with the inequality condition of Equation (13).

Example 5

The next example examined bichromatic waves consisting of two wave components. The first scenario has one component with a length equal to the ship length and another component that is longer. A threshold case was identified for a nominal (calm water) speed just below the occurrence of surf-riding (see Figure 14). In a bichromatic sea, the celerities of the two component waves, which are indicated by the red and green lines in Figure 14, define a celerity range that is obeyed only in the smoother regions of the curve of local celerity. Surge velocity came very close, yet did not cross the calculated celerity curve.

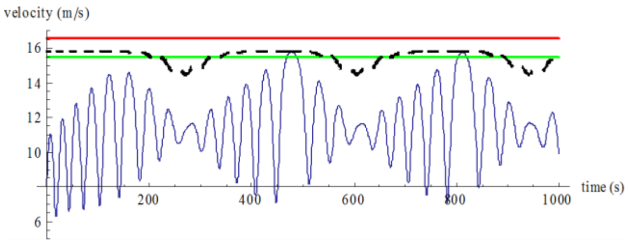

Figure 14: Surging in a bichromatic sea: ζ_1 = 2.5 m, λ = 175 m and ζ_2 = 3.4 m, λ = 152 m, (*Fn* = 0.28).

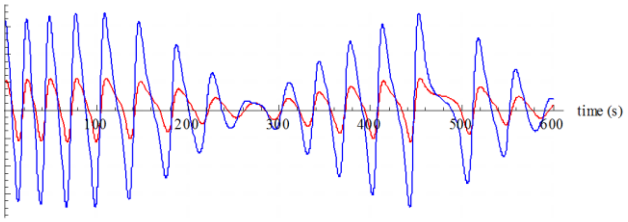

Figure 15: Phasing of wave slope (red) versus Froude-Krylov force (blue).

Figure 15 plots the time histories of Froude-Krylov surge force and the wave slope measured at the ship's instantaneous position. Figure 16 shows contours of the maxima of these quantities on a space-time plot. Both figures suggest that the maximum wave slope is, as expected, a good indicator of the maximum of the wave surging force.

The bichromatic wave simulation was then repeated using the same wave but with a slightly higher self-propulsion speed (Figure 17). This speed plot shows a crossing of the celerity curve, followed by ship motion with mean speed considerably higher than the self-propulsion speed and about the celerity value. This is realization of surf-riding. It is very noteworthy, however, that the observed motion has a persistently strongly oscillatory character.

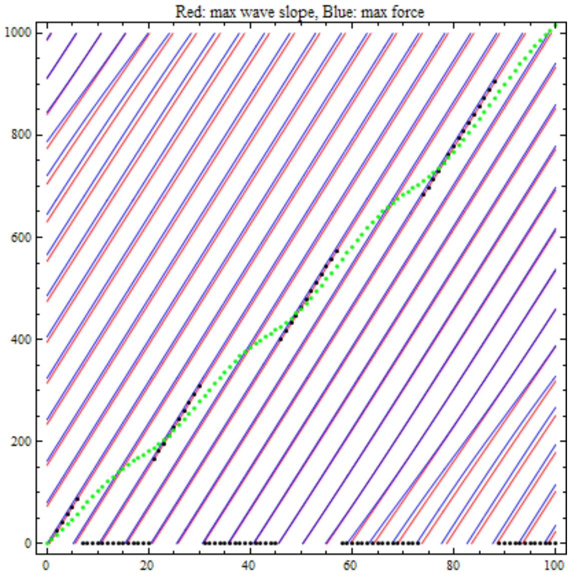

Figure 16: Space-time contour plot for maximum wave slope (red) and maximum force (blue). Green dots indicate the ship's instantaneous position. Blue dots show the identified nearest point of max slope for each ship position.

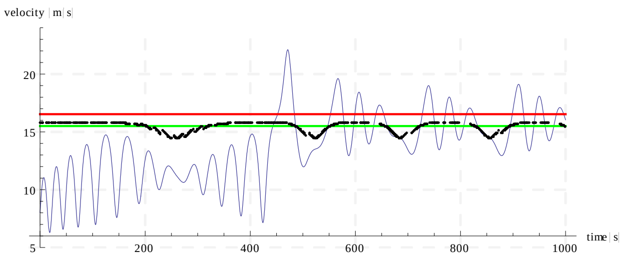

Figure 17: Threshold crossing at *Fn* = 0.283.

An additional bichromatic wave comprised of two long waves of moderate steepness produced a similar pattern. In Figure 18 the nominal speed is just below the surf-riding threshold, while in Figure 19 the nominal speed is just above the surf-riding threshold.

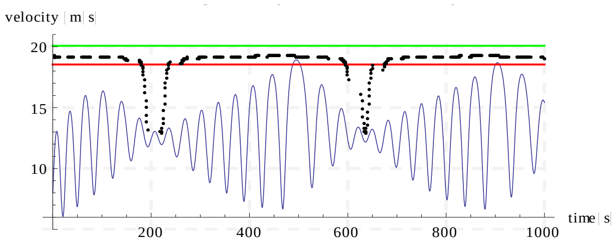

Figure 18: ζ_1 = 3.8 m, λ = 258 m and ζ_2 = 3 m, λ = 220 m and *Fn* = 0.315.

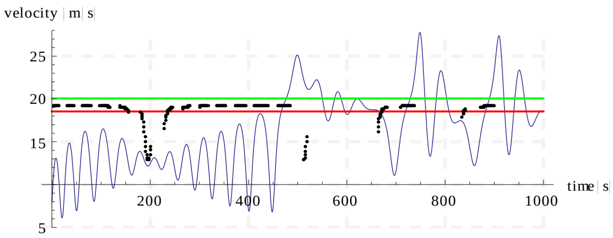

Figure 19: ζ_1 = 3.8 m, λ = 258 m and ζ_2 = 3 m, λ = 220 m and *Fn* = 0.319.

The Figure 19 scenario is also plotted in space-time for three different initial conditions, shown in Figure 20. Two of the resulting motion histories soon fall completely on each other, while the third does not. Despite this, the pattern of surf-riding behaviour exhibited in these results is identical. In the first two cases the ship is "caught" by the same wave while in the third case it is not caught by that wave but continues with ordinary surging until it is caught by a later wave.

Another noteworthy feature is seen from the trace of the curves on the time-space plane (Figure 21). While the lines of the two runs that show apparent surf-riding behaviour from the beginning are almost straight and indistinguishable, the third one has lower initial slope, which is indicative of the lower velocity of motion. However, it then “bends” and becomes parallel to the other two once the celerity threshold is exceeded and the ship is captured into surf-riding.

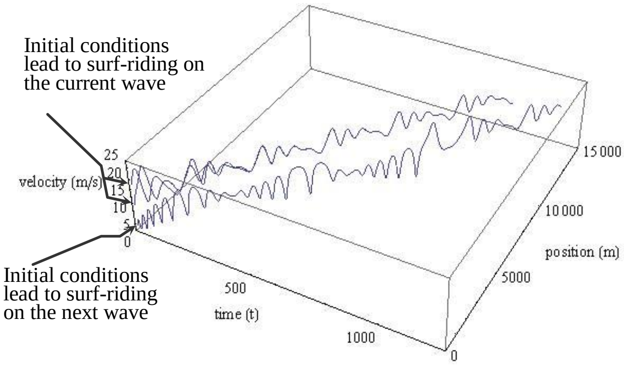

Figure 20: Realisations of surf-riding for different initial conditions (bichromatic wave).

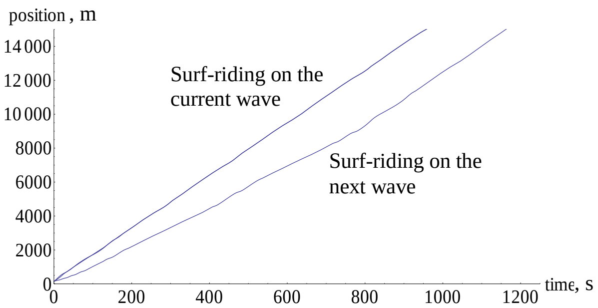

Figure 21: Traces of ship position curves on the time–space plane.

<u>Example 6</u>

The final example of the celerity calculation is an irregular sea case again based on the JONSWAP spectrum ($H_s = 3.5m, T_P = 10s$). The region of the spectrum at 5% around the peak frequency has been used, corresponding to wave lengths that are very close to the ship length (between 148 and 164 m). Wave realisations were based on six frequencies, with random phases. Ship behaviour for nominal speeds just below and well into the surf-riding regime are shown in Figures 22 and 23, respectively. For reference, the green line indicates the wave celerity corresponding to the mean wave frequency.

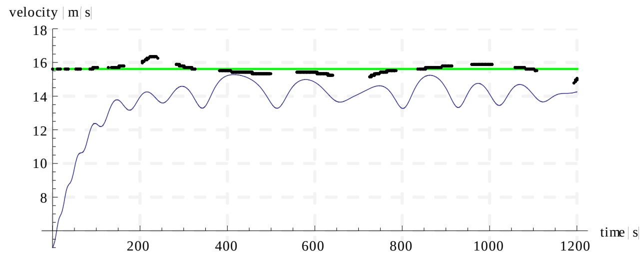

Figure 22: JONSWAP spectrum (*Fn* = 0.283).

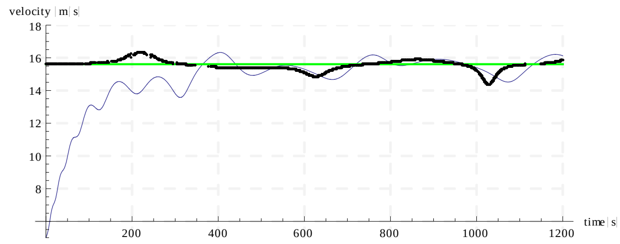

Figure 23: JONSWAP spectrum (*Fn* = 0.37) considering all max slopes (down and up).

As described above, the initial implementation of the celerity calculation only produced a result when the zero-slope point found near the ship was on the down slope. This results in the broken celerity curve in Figure 23. In Figure 24, the celerity calculation considers points on both the up and down slopes to produce a complete, though not necessarily continuous, curve.

5. LAMP IMPLEMENTATION

Following its initial verification using the 1-DOF model of surging, the irregular wave celerity calculation is being implemented in the Large Amplitude Motions Program (LAMP) where it will be used as part of a probabilistic model of surf-riding (Belenky et al. 2012). LAMP is a nonlinear time-domain computer simulation code for ship wave motions and loads that is built around a body-nonlinear 3-D potential flow solution of the wave-body hydrodynamic interaction problem and incorporates models for viscous, lift and propulsor effects. Previous studies have demonstrated that LAMP can simulate the principal phenomena of surf-riding and broaching-to (Spyrou et al. 2009).

The LAMP implementation of the wave celerity calculation generally follows the scheme described above, but has been adapted for LAMP's more general irregular wave models including oblique, short-crested (multi-direction) and nonlinear incident waves. The wave point that is tracked is the maximum wave slope in the direction of ship travel; it is tracked only in that direction, and the resulting wave celerity is calculated in this direction. In this manner, the tracked point is related to the force in the surging direction and the "celerity" characterizes the speed that the ship must reach, at its current heading, to stay at this point of maximum surging force. Note that this "directional" definition of celerity can be quite different from a "physical" wave celerity obtained by observing the motion of a wave feature from a global view point. In fact, for a ship travelling at an angle to long-crested seas, LAMP's "directional" celerity will be larger than the wave "physical" celerity, going to infinity in beam seas. However, this is correct for the consideration of surf-riding, as a ship would need to go infinitely fast to maintain its relative position to the crest or other feature of a beam wave.

Another difference in the LAMP implementation of the wave celerity calculation is that it always searches for the nearest maximum slope point on the down slope even if an up slope maximum is closer. This is done by pre-computing the elevation and its derivatives on a regular spatial interval δx_s in the travel direction and identifying intervals where a down-slope maximum can be found. A careful selection of the interval size can also significantly reduce the number of wave evaluations required to find and track the maximum slope points, which can be very important for wave models that include many components and/or nonlinear terms.

Figure 24 shows a snapshot of a LAMP simulation for the tumblehome hull form from the ONR Topsides series running in long-crested irregular waves. The plot shows the wave profile at that time instance along the ship's travel direction with marks for the points of maximum down slope and elevation (crest). The wave in this case is derived from a Bretschneider spectrum with H_s=7m and T_m12.0s.

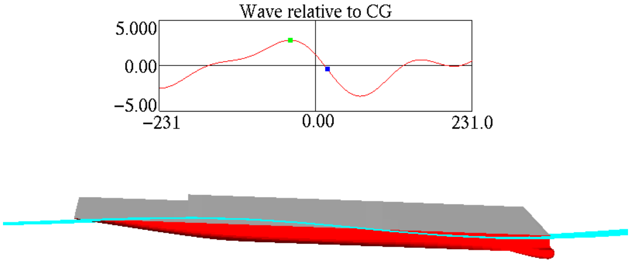

Figure 24: LAMP simulation of ONR Topsides tumblehome hull in irregular following seas.

Figures 25 and 26 show the time histories of the ship speed and the wave celerity for two different propeller rates.

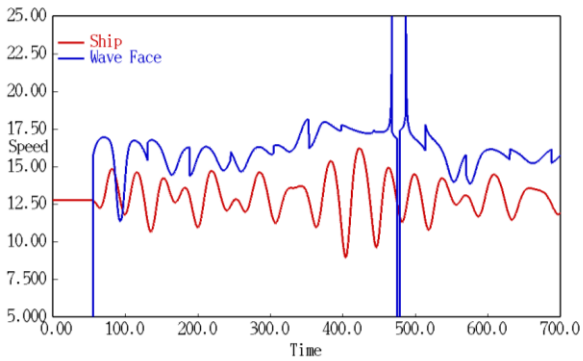

Figure 25: Ship speed and wave celerity for propeller speed of 2.2 rps.

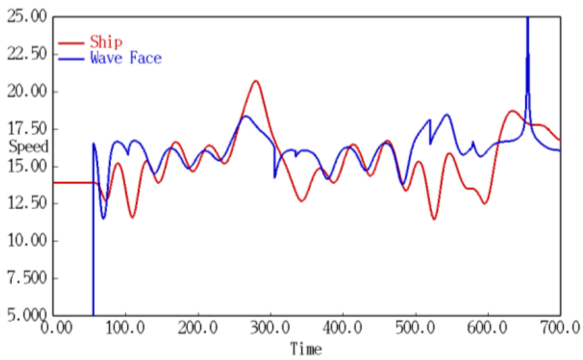

Figure 26: Ship speed and wave celerity for propeller speed of 2.4 rps.

At the lower propeller speed shown in Figure 25, the ship speed oscillates near its calm water speed and below the wave celerity, and no surf-riding is observed. At the higher propeller speed, there are three episodes where the ship's speed upcrosses the wave celerity and is captured into surf-riding for a period of time, matching the wave speed while surf-riding. While the initial wave celerity jump at 60 seconds is a plotting artifact, the other "spikes" in wave speed are cases where the phasing of the wave component produces a very rapid local translation of the point of maximum slope. At ~480s of the first record (Figure 25), an overtaking of one wave by a following one actual causes the maximum point to briefly slide back up the wave face and results in a negative celerity. The identification and handling of such situations is one objective of the current development. Despite these problem points, the present scheme seems to provide a practical calculation of wave celerity that is suitable for characterizing surf-riding in irregular waves.

6. CONCLUSIONS

In the development of a probabilistic model of surf-riding in irregular seas based on the time histories of wave elevation and ship motion, it has been proposed that the phenomena of surf-riding can be characterized by an up-crossing of the wave celerity by the ship speed. In order to implement such a scheme, it is necessary to calculate a relevant instantaneous wave celerity corresponding to the ship's position in the irregular wave at any given time. A scheme has been developed that calculates such a value by finding the point of maximum wave slope on the down slope of the wave nearest the ship and tracking its motion over a series of short time increments. The point of maximum slope has been selected because of its close relationship to the point of maximum wave surging force, which is a closely tied to surf-riding. The tracking scheme has been implemented and demonstrated in both a 1-DOF model of surging and in the LAMP 6-DOF time domain seakeeping code. Initial results indicate this scheme can reliably produce wave celerity values that can indeed be used to identify surf-riding in irregular waves.

7. ACKNOWLEDGMENTS

The research reported in this paper is funded by the Office of Naval Research (ONR) under Dr. Patrick Purtell and by ONR Global under Dr. Richard Vogelsong. This support is gratefully acknowledged by the authors.

8. REFERENCES

Aberg, S., and Rychlik, I., 2006, "Role of wave velocity for encountered wave statistics," Proceedings of the Sixteenth (2006) International Offshore and Polar Engineering Conference, San Francisco, California, May 28 - June 2.

Aberg, S., and Rychlik, I., 2007, "Doppler shift approximations of encountered wave statistics," Ocean Engineering, Vol. 34, 2300-2310.

Baxevani, A., Podgórski, K., and Rychlik, I., 2003, "Velocities for moving random surfaces", Probabilistic Engineering Mechanics, Vol. 18, 251-271.

Belenky, V.M., Spyrou, K.J., and Weems, K.M., 2012, "Evaluation of the Probability of Surf-Riding in Irregular Waves with the Time-Split Method," Proceedings of the 11th International Conference on the Stability of Ships and Ocean Vehicles (STAB 2012), Athens, Greece (to appear).

Boashash, B., 1992, "Estimating and Interpreting The Instantaneous Frequency of a Signal – Part 1: Fundamentals," Proceedings of the IEEE, Vol. 80, 520-538.

Gabor, D., 1946, "Theory of Communication," Journal of the IEE, Vol. 93, 429-457.

Kinsman, B., 1984, Wind Waves: Their Generation and Propagation on the Ocean Surface. Dover Publications Inc., New York, ISBN 0-486-64652-1.

Kratz, M.F., and León, J.R., 2005, "Curve crossings and specular points, d'apres Longuet-Higgins," www.mendeley.com/research/curve-crossings-specular-points-dapres-longuethiggins/#page-1.

Longuet-Higgins, M.S., 1957, "The Statistical Analysis of a Random, Moving Surface," Philosophical Transactions of the Royal Society of London. Series A, Mathematical and Physical Sciences, Vol. 249, 966, 321-387.

Mandel, L., 1974, "Interpretation of instantaneous frequency," American Journal of Physics, Vol. 42, 840-846.

Pierson, W.J., Jr., 1955, "Wind-generated gravity waves", in Advances in Geophysics, Vol. 2, Academic Press Inc. (New York), 93-178.

Spyrou, K.J., 2006, "Asymmetric surging of ships in following seas and its repercussions for safety", Nonlinear Dynamics (ed. A.H. Nayfeh), Kluwer, Vol. 43, 149-272.

Spyrou, K.J, Weems, K.M., and Belenky, V., 2009, "Patterns of Surf-Riding and Broaching-to Captured by Advanced Hydrodynamic Modelling," Proceedings of the 10th International Conference on Stability of Ships and Ocean Vehicles (STAB2009), St. Petersburg, Russia.

Vossers, G., 1962, "Behaviour of Ships in Waves," Volume IIC of Ships and Marine Engines, The Technical Publishing Company H. Stam N.V., Harlem, Netherlands.